

Targeted Deletion of Protein Kinase C λ Reveals a Distribution of Functions between the Two Atypical Protein Kinase C Isoforms¹

Rachel S. Soloff,^{2*†} Carol Katayama,^{*†} Meei Yun Lin,^{*†} James R. Feramisco,^{†‡§} and Stephen M. Hedrick^{3*†¶}

Protein kinase C λ (PKC λ) is an atypical member of the PKC family of serine/threonine kinases with high similarity to the other atypical family member, PKC ζ . This similarity has made it difficult to determine specific roles for the individual atypical isoforms. Both PKC λ and PKC ζ have been implicated in the signal transduction, initiated by mediators of innate immunity, that culminates in the activation of MAPKs and NF- κ B. In addition, work from invertebrates shows that atypical PKC molecules play a role in embryo development and cell polarity. To determine the unique functions of PKC λ , mice deficient for PKC λ were generated by gene targeting. The ablation of PKC λ results in abnormalities early in gestation with lethality occurring by embryonic day 9. The role of PKC λ in cytokine-mediated cellular activation was studied by making mouse chimeras from PKC λ -deficient embryonic stem cells and C57BL/6 or *Rag2*-deficient blastocysts. Cell lines derived from these chimeric animals were then used to dissect the role of PKC λ in cytokine responses. Although the mutant cells exhibited alterations in actin stress fibers and focal adhesions, no other phenotypic differences were noted. Contrary to experiments using dominant interfering forms of PKC λ , mutant cells responded normally to TNF, serum, epidermal growth factor, IL-1, and LPS. In addition, no abnormalities were found in T cell development or T cell activation. These data establish that, in vertebrates, the two disparate functions of atypical PKC molecules have been segregated such that PKC ζ mediates signal transduction of the innate immune system and PKC λ is essential for early embryogenesis. *The Journal of Immunology*, 2004, 173: 3250–3260.

The protein kinase C (PKC)⁴ superfamily is composed of 10 individual serine/threonine kinases, which are encoded by nine different genes (1). These kinases share sequence and structural homology, but vary in their activation requirements and tissue expression. They can be divided into three groups based on sequence homology and biochemical regulation, specifically the requirement for the second messengers calcium and diacylglycerol. The classical isoforms α , β 1, β 11, and γ are dependent on both second messengers, whereas the novel isoforms δ , ϵ , η , and θ do not require calcium for their activation. The third group, the atypical isoforms ζ and λ (ι in humans) (also referred to as aPKCs), do not use calcium or diacylglycerol for their activation. The method of their activation is unclear, but may involve

lipid metabolites of PI3K, which includes 3,4,5-phosphatidylinositol triphosphate (2–4).

The two atypical isoforms, ζ and λ , are 72% identical at the amino acid level (3, 5). The most similar region of homology is within the kinase domain at the carboxy terminus, suggesting similar or identical substrates. Several commonly used Abs bind to this region (6, 7); therefore, in many studies the isoform being studied, ζ or λ , is difficult to discern. Northern blot analysis of mRNA expression suggests that PKC λ has a wider tissue distribution than does PKC ζ and is the predominant isoform expressed in the thymus (8), fetal heart (9), colon cell extracts (10), and the leukemic cell line K562 (11). The function of both aPKC family members is abrogated by the same pseudosubstrate inhibitor (12, 13), thus further hampering the ability to assign unique functions to the individual enzymes.

Using the pseudosubstrate inhibitor as well as kinase-dead or active forms of the proteins, the aPKCs have been implicated in cell proliferation and survival. Induction of the ERK after treatment with serum or TNF can be inhibited by overexpression of catalytically inactive forms of either aPKC (14, 15). Induction of a 12-*O*-tetradecanoyl-phorbol-13-acetate response element by epidermal growth factor (EGF) or platelet-derived growth factor can also be blocked by overexpression of an inactive aPKC (4). Similar types of experiments suggest that PKC λ and ζ both activate NF- κ B after TNF treatment (16–18), and this is supported by experiments using cells from mice deficient in PKC ζ (19). The role of PKC λ in this pathway is still in question. The aPKC isoforms have also been shown to protect cells from apoptosis through the induction of NF- κ B. PKC ζ -deficient mouse embryonic fibroblasts (MEFs) are more sensitive to apoptosis induced by TNF and cycloheximide (19). In the absence of aPKC function, colon cancer cells appear to be more susceptible to apoptosis induced by chemotherapeutic

*Division of Biological Sciences, [†]Moores University of California at San Diego Cancer Center, [‡]Department of Medicine, [§]Department of Pharmacology, and [¶]Department of Cellular and Molecular Medicine, University of California at San Diego, La Jolla, CA 92093

Received for publication April 14, 2004. Accepted for publication June 17, 2004.

The costs of publication of this article were defrayed in part by the payment of page charges. This article must therefore be hereby marked *advertisement* in accordance with 18 U.S.C. Section 1734 solely to indicate this fact.

¹ This work was supported by Public Health Service Grant AI21372-21 (to S.M.H.) and National Cancer Institute Cancer Center Grant P30 CA23100 (to J.R.F.). R.S.S. was supported by The Jane Coffin Childs Memorial Fund for Medical Research and the California Division of the American Cancer Society (Fellowship 1-30-99).

² Current address: Gemini Science, 10355 Science Center Drive, San Diego, CA 92121.

³ Address correspondence and reprint requests to Dr. Stephen M. Hedrick, Department of Biological Sciences, University of California at San Diego, 9500 Gilman Drive, La Jolla, CA 92093-0377. E-mail address: shedrick@ucsd.edu

⁴ Abbreviations used in this paper: PKC, protein kinase C; aPKC, atypical PKC; EGF, epidermal growth factor; MEF, mouse embryonic fibroblast; PAR, partition defective; Par, prostate apoptosis response; ES cell, embryonic stem cell; TA_g, SV40 large T-antigen; NA, numerical aperture.

agents (11), and up-regulation of PKC λ expression correlates with colon cancer progression (10).

The aPKCs are most variable at the amino-terminal regulatory domain, including several protein interaction sequences. This suggests that PKC λ and ζ may interact with different proteins. The N-terminal region of aPKC has been recognized as belonging to a domain family termed the PB1 domain (Phox and Bem1p) (20). This domain has been found in a number of proteins including Bem1p, which mediates cell polarity in budding yeast; partition defective (PAR)-6, which mediates asymmetric cell divisions and embryonic polarity in *Caenorhabditis elegans* (21, 22); mammalian p40^{phox} and p67^{phox} proteins, which activate the phagocyte microbicidal NADPH oxidase (20); and p62/ ζ -interacting protein, which mediates the activation of NF- κ B via various cell surface receptors (23, 24). Each of these signaling molecules has been shown to exist as a complex formed by homotypic interactions with PB1-containing proteins, including the aPKCs (25, 26).

Also in the N-terminal region of aPKC is a proline-rich PXXP domain that mediates interactions with Src homology domain 3 (SH3) domains upon activation with nerve growth factor (27). This interaction results in the phosphorylation of at least three tyrosines in the catalytic domain, one of which appears to be important in the regulation of PKC λ . A third amino acid sequence motif in the regulatory domain is a cysteine-rich domain termed C1, and this has been reported to interact with prostate apoptosis response-4 (Par-4; not *C. elegans* PAR-4) in the regulation of apoptosis (28, 29). Both the PKC ζ and PKC λ molecules have been shown to prevent Par-4-mediated apoptosis in a kinase-dependent manner.

Finally, PAR-3, another molecule important in the establishment of embryonic polarity, associates with aPKCs through the catalytic domain. PAR-3, PAR-6, and aPKC colocalize to one pole of the asymmetrically dividing blastomeres, and the diminished

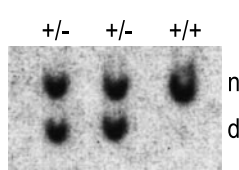
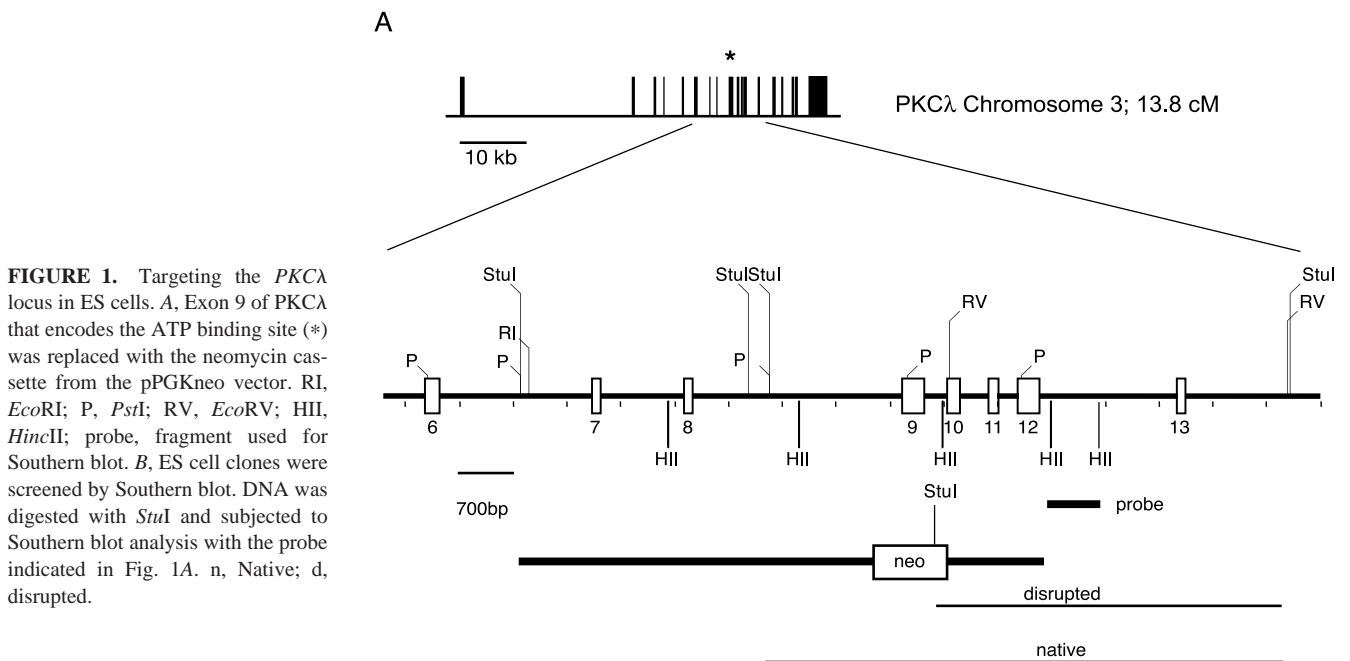
expression of any one of these molecules reveals a partition-defective phenotype (30).

To directly assess the unique functions of PKC λ in mice, PKC λ -deficient mice were generated by gene targeting. We found that the absence of PKC λ during gestation results in early embryo lethality, but it is not involved in TNF-mediated signal transduction leading to the activation of MAPK or NF- κ B.

Materials and Methods

Production of PKC λ -deficient mice

Since the initiation of this project, the mouse genome project made the entire sequence of the PKC λ locus available for analysis, and a schematic diagram of the exon-intron structure is shown in Fig. 1A. The asterisk denotes that exon 9 encodes the ATP-binding site of the catalytic domain. The exons encoding the kinase domain of PKC λ were mapped from genomic clones isolated from a 129SvJ library (Stratagene, La Jolla, CA). The probe used was the full-length PKC λ cDNA isolated by RT-PCR from thymocyte RNA. Similar to the targeting strategy used for other PKC family members, exon 9 containing the ATP binding site and the intron between exons 9 and 10 including the splice acceptor site for exon 10 were replaced with the pGK-neo cassette (31) in the opposite transcriptional orientation (Fig. 1A). The targeting construct was linearized with *Sall* and transfected into the R1 embryonic stem cell (ES cell) line by electroporation. Transfected cells and the resulting clones were grown on neomycin-resistant mouse embryonic fibroblasts that were inactivated with mitomycin C or irradiated at 30 G. PKC λ -deficient clones were identified by digesting genomic DNA with *StuI* and were screened with a radiolabeled *HincII* fragment from a region flanking the 3' end of the deletion (Fig. 1B). Recombinant clones were injected into C57BL/6 blastocysts or RAG2-deficient blastocysts, and chimeric mice were backcrossed to C57BL/6 mice or were analyzed directly. DNA was isolated from tail snippets of agouti pups and screened as described above to identify mice hemizygous for the PKC λ disruption. For some experiments, liver from embryonic day 16 embryo chimeras was harvested and used to reconstitute irradiated C57BL/6 mice. The radiation chimeras were tested for immune development and T cell activation 6–12 wk after reconstitution.



Mice

The mice were generated at the University of California, San Diego Transgenic Core Facility, bred, and maintained in the University of California, San Diego animal facilities (La Jolla, CA). Timed matings were set up by placing one male in a cage with two or three females for 16 h. The presence of a vaginal plug was considered day 1 of gestation.

Screening of embryos

Day 6–9.5 embryos were dissected from deciduas, photographed, and digested at 55°C overnight in lysis buffer composed of 10 mM Tris-Cl (pH 8.3), 2 mM MgCl₂, 0.1 mg/ml gelatin, 0.45% Nonidet P-40, 0.45% Tween 20, and 10 μ g/ml proteinase K. The samples were then heated to 95°C for 10 min and the DNA was directly used in PCRs to determine the genotype. PCRs were performed in 50- μ l volume with a final concentration of 1.5 mM Mg²⁺, 200 μ M nucleotides, 2.5 U of *Taq*DNA Polymerase (Invitrogen, Carlsbad, CA), and 250 ng of each primer, L5' endo, L3' endo, and Neo3'S3. The PCR protocol was 35 cycles of 1 min at 94°C, 1 min at 58°C, and 1 min 20 s at 72°C, with a final 7-min incubation at 72°C. One-fifth of the amplified material was resolved through a 2% Nusieve 3:1 agarose gel (BioWhittaker, Walkersville, MD) containing ethidium bromide.

Preparation and analysis of RNA

Total RNA was prepared using Trizol reagent (Invitrogen) following the manufacturer's protocol. For Northern blot analysis, 10 μ g of total RNA was resolved through a 1% formaldehyde gel, transferred to Duralon nylon membrane (Stratagene), and hybridized to a radiolabeled PKC α -specific probe corresponding to the 5' end of the cDNA. For RT-PCR analysis, total RNA was converted to cDNA with avian myeloblastosis virus reverse transcriptase (Promega, Madison, WI), and cDNA was amplified in a 50- μ l buffered solution containing 1–1.5 mM Mg²⁺, 200 μ M nucleotides, 2.5 U of *Taq*DNA polymerase (Invitrogen), and 250 ng of each primer. The individual cycles were 30 s at 94°C, 1 min at 58°C, and 2 min at 72°C, repeated 35 times with a final extension of 7 min at 72°C. One-fifth of the amplified material was resolved through an agarose gel containing ethidium bromide. Real-time PCR was performed on cDNA using the Brilliant SYBR Green system (Stratagene) and was analyzed on the MX4000 (Stratagene). The thermal profile was as follows: an initial melt of 10 min at 95°C, then 40 cycles of 30 s at 95°C, 1 min at 55°C, and 30 s at 72°C. Finally, a melting segment was performed to determine the purity of the PCR product. For normalization, reactions were included using primers for acidic ribosomal protein. Expression of exons 1–2, exon 9, and exons 12–14 was measured.

Oligonucleotides

The oligonucleotides used in this study were synthesized by GENSET (La Jolla, CA), GenBase (La Jolla, CA), or Integrated DNA Technologies (Coralville, IA) and are listed beginning at the 5' end: L5' endo (AACACCAGGGAGAGTGG), L3' endo (GCCTAGAAAGTAACCCAC), Neo3'S3 (GACGAGTTCTTCTGAGGGG), mouse PKC α 5' (GTGAGG AGATGCCGACCCAG), mouse PKC α 3' (CTGACGGGTGGATATC CATG), β -actin5 (GTGGGCCGCTCTAGGCACCAA), β -actin3 (CTCTTT GATGTCACGCACGAT), PKC α -ex1-5' (GGGTGAAAGCCTACTACCG), PKC α -ex2-3' (TGCTCATTTGTCAAAGAACAC), PKC α -ex9-5' (CTAG GTCTGCAGGATTTCG), PKC α -ex9-3' (TTGACGAGCTCTTCTTCAC), PKC α -ex12-5' (CTACGGCATGTGTAAGGAA), PKC α -ex14-3' (CAAC GATATCAAACGGAGAC), PKC α -ex6-3' (CCCACACTCAATTGT GACC), PKC α -ex8-3' (ACCAACTTGGTCCAAACTCT), PKC α -ex18-3' (TCAGACACACTTCTGTC), acidic ribosomal protein-left (CGACCTG GAAGTCCAACTAC), and acidic ribosomal protein-right (ATCTGCTGC ATCTGCTTG).

In situ hybridization

Day 16 embryos were rapidly frozen in Tissue-Tek OCT (VWR International, West Chester, PA) by using liquid nitrogen. Serial sagittal sections (20 μ m) were cut, thaw-mounted onto charged microscope slides, fixed, and processed by standard methods (32). Digoxigenin-labeled PKC α -specific riboprobes were transcribed in the sense and antisense orientations from linearized PKC α 5' plasmid by using the DIG RNA labeling kit (Boehringer Mannheim, Indianapolis, IN). Hybridization was conducted by using 2 ng/ μ l labeled riboprobe in hybridization solution (50% formamide, 2 \times standard saline citrate phosphate/EDTA, 10 mM DTT, 2 mg/ml yeast tRNA, 0.5 mg/ml polyadenylic acid, 2 mg/ml BSA Fraction V (Sigma-Aldrich, St. Louis, MO), and 0.5 mg/ml salmon sperm DNA) for 12–16 h at 65°C. Slides were washed twice at room temperature for 45 min in 2 \times standard saline citrate phosphate/EDTA/0.6% Triton X-100, followed by three 30-min washes at 65°C in high-stringency buffer (2 mM Na₄P₂O₇, 1

mM Na₂HPO₄, and 1 mM sodium-free EDTA (pH 7.2)). After washes, slides were incubated in 1% blocking buffer (Boehringer Mannheim) in 0.3% Triton X-100 in TBS for at least 1 h, followed by overnight incubation with anti-digoxigenin-alkaline phosphatase F(ab')₂ (Boehringer Mannheim) at 1/500 in blocking buffer. Slides were washed in TBS and then processed for colorimetric detection with NBT and 5-bromo-4-chloro-3-indolyl-phosphate. Slides were counterstained with Nuclear Fast Red (Vector Laboratories, Burlingame, CA) and then were examined microscopically.

MEF isolation

Chimeric embryos were dissected at days 13–15. The head and internal organs were removed and the remaining tissue was minced with scissors and then passed through an 18-gauge needle until a single cell suspension was formed. Four embryos were processed at one time and the resulting cells were seeded into a 15-cm tissue culture dish containing 25 ml of complete medium (DMEM high glucose supplemented with 10% FCS (HyClone, Ogden, UT), 2 mM glutamine, 1000 U/ml penicillin/streptomycin, 100 mM sodium pyruvate, 1 \times nonessential amino acids, and 5 \times 10⁻⁵ 2-ME). When the cells reached confluency, they were harvested with trypsin and five vials/plate were frozen. The passage 2 cells were then treated with 400 μ g/ml Geneticin (G418) (Invitrogen) until individual colonies grew out. The resulting MEF cell lines were analyzed by PCR and Western blot analysis to determine the genotype and presence or absence of the PKC α protein, respectively. In all of the experiments described, the selected MEFs were between passages 3 and 6.

Immortalization of MEFs

Passage 2 MEFs were seeded in 10-cm dishes at 5 \times 10⁴ cells per dish in 10 ml of complete medium. The next day, DNA-calcium phosphate precipitates, each containing 10 μ g of salmon sperm DNA and 1 μ g/ml SV40 large T-antigen (TAG) expression plasmid, pselectESV (a gift from M. J. Tevethia, Pennsylvania State University College of Medicine, Hershey, PA), were prepared as described (33). One milliliter of the precipitate was added directly to the medium in each dish of MEFs. After overnight incubation at 37°C, the medium was replaced with fresh complete medium. When the cells formed a monolayer, they were removed by trypsin treatment and one-tenth of the resulting cell suspension was transferred to a new dish containing complete medium. Each time a confluent monolayer was formed, the culture was split 1:10 for 10 consecutive passages, at which point they were considered an immortal cell line.

Western analysis

MEFs were washed in PBS and lysed in Triton X-100 buffer (1% Triton X-100, 10 mM Tris (pH 7.5), 150 mM NaCl, 200 μ M sodium vanadate, 1 μ g/ml aprotinin, 1 μ g/ml leupeptin, and 1 mM PMSF). Protein concentration was determined by the Bio-Rad protein assay (Bio-Rad, Hercules, CA). Equivalent amounts of protein were separated by 12% SDS-PAGE (Bio-Rad Ready gels) and transferred to Immobilon membranes (Millipore, Bedford, MA). Membranes were blocked in TBST (0.1% Tween 20) with 5% nonfat milk and were incubated with anti-phospho-MAPK (New England Biolabs, Beverly, MA), anti-ERK2 (C-14; Santa Cruz Biotechnology, Santa Cruz, CA), anti-PKC α (610208; BD Transduction Laboratories, Lexington, KY), anti-PKC α (Invitrogen), anti-PKC θ , anti-I κ B α (Santa Cruz Biotechnology), or anti-PKC ζ (07-264; Upstate Biotechnology, Lake Placid, NY) in TBST, 5% milk. Blots were then incubated with horse anti-rabbit or horse anti-mouse HRP secondary Abs (Vector Laboratories) and developed using ECL (Amersham, Piscataway, NJ).

Analysis of PKC translocation in thymocytes

Thymocytes from AND TCR transgenic mice on the IA^k background (34) were stimulated for 30 min with DCEK APCs \pm 2 μ M pigeon cytochrome *c* peptide. Isolation of the cytoplasmic and membrane fractions was performed as described by Isakov and Altman (35). Briefly, the cells were washed with cold PBS and then resuspended in lysis buffer A (20 mM Tris-HCl (pH 7.5), 0.25 M sucrose, 10 mM EGTA, 2 mM EDTA, 1 mM PMSF, 20 μ g/ml leupeptin, and 10 μ g/ml aprotinin) at a concentration of 5 \times 10⁶/ml. The cells were disrupted by sonication for 2 min in 15-s pulses. The homogenized cells were centrifuged at 100,000 \times g for 1 h at 4°C. The supernatant from this centrifugation was used as the cytosolic fraction. The pellet was then resuspended in lysis buffer A with 1% Triton X-100. After a 30-min incubation on ice, the lysates were spun a second time at 100,000 \times g for 1 h at 4°C. The supernatant was used as the membrane fraction. The fractions were then analyzed by Western blot.

T cell proliferation assays

Ninety-six-well U-bottom plates were coated with goat anti-hamster Ig (Southern Biotechnology Associates, Birmingham, AL) in carbonate buffer (pH 9.5) for 1 h at 37°C. The wells were washed with PBS, and anti-mouse CD3 ϵ (145-2C11) was added in medium at the indicated concentrations and incubated for 1 h at 37°C. After washing with PBS, soluble anti-mouse CD28 hybridoma supernatant was added to some wells. In other wells, 100 U/ml recombinant human IL-2 (Hoffmann-LaRoche, Nutley, NJ) was added. Total splenocytes were added at 2×10^5 /well in a final volume of 200 μ l. Cultures were incubated at 37°C with 5% CO₂ for a total of 72 h. Tritiated thymidine (0.5 μ Ci; PerkinElmer Life Sciences, Wellesley, MA) was added to each well in a volume of 10 μ l for the last 18 h of culture. Incorporated thymidine was measured by harvesting the cultures onto glass fiber mats and counting by liquid scintillation.

Immunofluorescence and deconvolution microscopy

Cells were plated at 5×10^4 cells per well of a six-well dish in complete medium. Each well contained four 12-mm glass coverslips. The cells were allowed to settle and grow for 48 h. For analysis of tubulin, two coverslips of each genotype were removed and dipped in ice-cold methanol for 5 s, rinsed in water for 5 s, and transferred to PBS. For analysis of actin, vimentin, and paxillin, the coverslips were rinsed with PBS and then incubated with 3.7% formaldehyde in PBS for 10 min, followed by two more washes with PBS before extraction with 0.3% Nonidet P-40 detergent in PBS. Fluorescently labeled phalloidin (Sigma-Aldrich) was used to visualize F-actin, while indirect immunofluorescence was conducted using Abs specific for paxillin, vimentin (both from Santa Cruz Biotechnology), and tubulin (a gift from D. W. Cleveland, University of California at San Diego). The nucleus was visualized with 4',6'-diamidino-2-phenylindole or Hoescht (Sigma-Aldrich).

Deconvolution microscopy was conducted at the Moores University of California at San Diego Cancer Center Digital Imaging Shared Resource (La Jolla, CA). Images were captured with a DeltaVision deconvolution microscope (Applied Precision, Issaquah, WA) (36). The system uses a charge-coupled device camera (Photometrics, Tucson, AZ) mounted on a Nikon TE-200 microscope (Melville, NY). In general, 20 optical sections spaced by 0.2 μ m were taken. Intensities were kept in the linear range of the camera. Lenses included $\times 100$ (numerical aperture (NA) 1.4), $\times 60$ (NA 1.4), and $\times 40$ (NA 1.3). The data sets were deconvoluted and analyzed using SoftWorx software (Applied Precision) on a Silicon Graphics Octane workstation (Mountain View, CA). Volume views using maximal projections are shown as indicated.

ERK stimulation

Immortalized fibroblasts were plated at 5×10^5 cells per 10-cm dish in complete medium. One dish per condition was set up. After 24 h, the medium was removed and the cells were washed with medium lacking serum. Medium with 0.5% platelet-poor human serum was added to the dishes and the cells were incubated for 48 h at 37°C with 5% CO₂. The medium was then replaced with fresh low serum medium plus one of the following stimuli: murine TNF- α (10 ng/ml; R&D Systems, Minneapolis, MN), EGF (100 ng/ml), platelet-derived growth factor (100 ng/ml), or PMA (10 ng/ml) (all from Sigma-Aldrich) plus the calcium ionophore A23187 (Calbiochem, San Diego, CA). The cells were then incubated for 15 min or for a time course from 0 to 20 min at 5-min intervals. The medium was removed and replaced with cold PBS. The cells were scraped on ice and transferred to Eppendorf tubes for lysis. Western blots were performed using anti-ERK1&2 and anti-ERK2.

Reporter assays

MEFs were seeded in 12-well plates at 7×10^4 cells/well in complete medium containing 10% FCS. Eighteen hours later, the cells were transfected with p3(HIV) κ B-luciferase (a gift from C. Hauser, The Burnham Institute, La Jolla, CA) and renilla luciferase encoding plasmid (Promega) using Superfect (Qiagen, Valencia, CA). The next day, the cells were washed with HBSS and the medium was replaced with medium containing 0.5% serum. Twenty-four hours later, the cells were stimulated with murine TNF (10 ng/ml), murine IL-1 β (100 ng/ml; R&D Systems), LPS (100 ng/ml; Sigma-Aldrich), or PMA (10 ng/ml; Sigma-Aldrich) for 2 h. They were then washed with PBS, lysed, and analyzed using the Dual Luciferase Reporter System (Promega). Luciferase activity was determined on a Moonlight 2010 luminometer (Analytical Luminescence Laboratory, San Diego, CA).

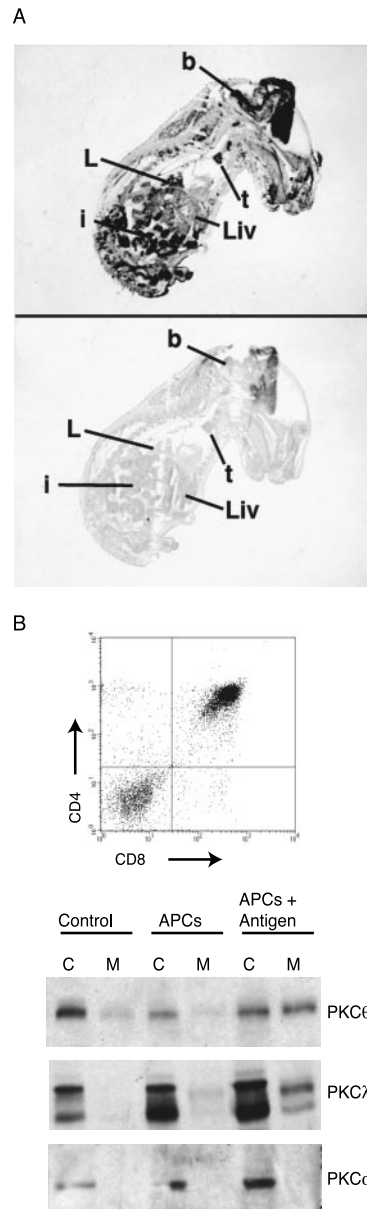


FIGURE 2. PKC λ expression and activation in the thymus. *A*, The tissue distribution of PKC λ in day 16 wild-type embryos was determined by in situ hybridization on adjacent frozen sections with a PKC λ antisense riboprobe (*top panel*) or sense riboprobe (*bottom panel*). b, Brain; i, intestine; L, lung; Liv, liver; t, thymus. *B*, PKC λ is translocated in response to Ag stimulation of thymocytes. Thymocytes were isolated from AND TCR transgenic mice crossed to express H-2A^k. In the absence of positive selection, developmental progression is blocked such that 95% of the cells exhibit a CD4⁺CD8⁺ phenotype. This population was cultured alone (Control), with APCs, or with APCs plus a peptide of pigeon cytochrome c, the Ag to which AND thymocytes respond. Cells were lysed by sonication in the absence of detergent, and membrane (m) and cytoplasmic (c) fractions were separated by centrifugation at 100,000 \times g. The membrane fraction-containing pellet was then solubilized with Triton X-100. Lysates were subjected to Western blotting using Abs specific for PKC θ , the atypical PKCs (λ and ζ), and α .

Results

Expression and activation of PKC λ

The expression pattern of PKC λ in late gestation mouse embryos was determined by in situ hybridization with a PKC λ -specific riboprobe (Fig. 2). In agreement with Akimoto et al. (3), PKC λ is

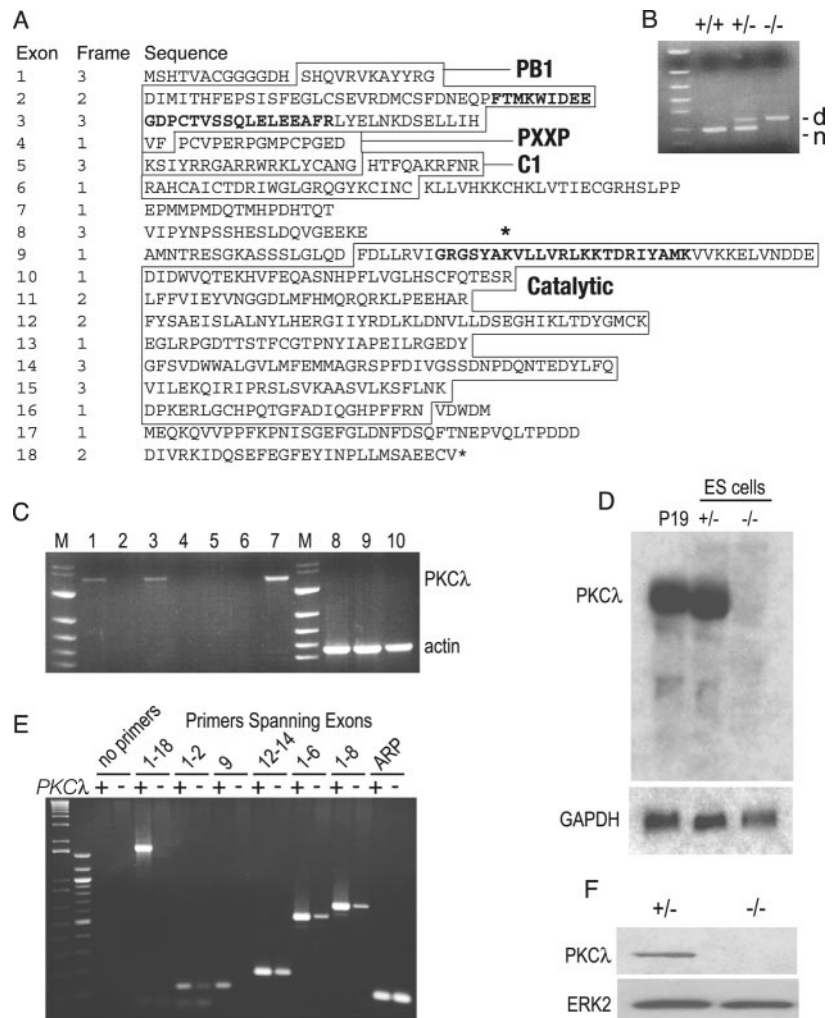
expressed at low levels in most tissues. High expression was found in the brain, thymus, lung, and intestine. To determine whether PKC λ is functionally responsive to activation through the T cell Ag receptor, we examined one parameter of activation, translocation from a free cytoplasmic form to a form associated with subcellular membrane components (37). To analyze this, thymocytes from TCR transgenic mice were isolated and cultured with or without Ag stimulation. The population analyzed was 95% CD4⁺CD8⁺ immature thymocytes with no appreciable subset of mature CD4⁺ or CD8⁺ T cells (Fig. 2B, upper panel). Cytoplasmic and membrane fractions from this population were subjected to immunoblotting for three PKC isoforms, α , θ , and λ . Most of the PKC was detectable in the cytoplasmic fraction in unstimulated thymocytes or in thymocytes cocultured with APCs alone. In thymocytes cultured with APCs and Ag, PKC θ and λ , but not α , were translocated to the membrane fraction. Although there are two bands developed using an anti-aPKC Ab, PKC ζ is expressed at very low levels in thymocytes and it is possibly undetectable. Furthermore, PKC λ and PKC ζ have virtually identical molecular weights, so it is likely that PKC ζ would be obscured by PKC λ . This is clear from experiments described below using PKC λ -deficient cells, but it illustrates the difficulty in distinguishing these two isoforms. These experiments combined with experiments showing that PKC λ can mediate survival through NF- κ B activation suggested that PKC λ may play a role in T cell development and activation. To study a role of PKC λ in embryogenesis and immune function, we generated mice deficient for PKC λ .

PKC λ -deficient mice

The murine PKC λ cDNA was isolated from thymocyte RNA by RT-PCR and was sequenced. The entire cDNA was used to screen an isogenic 129SvJ genomic library. Six overlapping genomic clones were identified, and part of the locus was mapped (Fig. 1A). Using the now available mouse genome data analyzed by the University of California, Santa Cruz, and the National Center for Biotechnology Information, the relationship between the gene structure and the protein domain structure was determined (Fig. 3A). Exons 1, 2, and 3 encode the PB1 domain, and exons 4, 5, and 6 encode the PXXP and C1 domains. The catalytic site of the kinase domain is encoded within exon 9, whereas the kinase domain is encoded by exons 9–16. Curiously, there is no apparent segregation of these protein motifs to individual exons, even though these domains have been conserved throughout eukaryotes.

The targeting strategy ablated exon 9, as well as the intron between exons 9 and 10 (including the splice acceptor site to exon 10) (Fig. 1A), thus preventing any possibility for kinase activity (38). In the absence of exon 9 and the splice acceptor for exon 10, this strategy also prevents translation of any sequences downstream of the kinase catalytic site. Exon 8 is in a different translational register from exon 11 (Fig. 3A). A further implication is that a resulting message would be subject to RNA degradation due to nonsense-mediated decay (39); however, the possibility exists that a transcript including exons 1–8 in frame could be processed into mRNA and translated to produce an N-terminal polypeptide that includes the PB1, PXXP, and C1 domains.

FIGURE 3. Analysis of PKC λ -deficient mouse embryos and ES cells. **A**, Using data from the mouse genome project compiled and annotated by the University of California, Santa Cruz, and the National Center for Biotechnology Information, the PKC λ locus was analyzed for the relationship between intron-exon structure and protein sequence. **A**, The exon number and reading frame are listed, and the protein domains are boxed. The bold amino acid subsequence in the PB1 domain represents the acidic subsequence termed OPR/PC/AID. The bold sequence in the catalytic domain represents the catalytic site with the ATP-binding lysine identified by an asterisk. **B**, PCR genotyping of day 8.5 embryos from mating of PKC λ heterozygotes. d, Disrupted; n, native. **C**, RT-PCR was used to analyze expression of PKC λ in day 7.5 embryos. The PKC λ specific product corresponded to the genotype (data not shown). Controls included no reverse transcriptase (lanes 2, 4, and 6) amplification of actin in the samples from each of the mice (lanes 8–10) and total RNA from P19 cells (lane 7). M, Molecular mass markers. **D**, Total RNA was isolated from P19, an embryonic carcinoma cell line, hemizygous (+/-), and homozygous PKC λ -deficient (-/-) ES cells and was analyzed by Northern blot with a 5' PKC λ -specific cDNA probe. **E**, RNA was isolated from wild type (+) or PKC λ -deficient (-) TAG MEFs and subjected to RT-PCR using primer pairs that span multiple exons, as indicated. Acidic ribosomal protein (ARP) represents primers that are specific for acidic ribosomal protein. **F**, Whole cell extracts from PKC λ hemizygous (+/-) or homozygous deficient (-/-) primary MEFs were analyzed by Western blot analysis with a PKC λ -specific Ab and an ERK2-specific Ab as a loading control.



The final construct was transfected into R1 ES cells, and after selection with G418, individual clones were screened by Southern blot for homologous recombination of the neo gene into the *PKC λ* locus. Six independent clones of 200 were identified as homologous recombinants, and two of these clones were independently injected into blastocysts from C57BL/6 mice. Twenty-one chimeric mice were generated, and 12 were bred to C57BL/6 mice, of which nine transmitted the knockout allele to their offspring. Subsequent breeding of the phenotypically normal heterozygous mice resulted in offspring of wild-type or heterozygous genotype at the expected Mendelian ratio (Table I). However, from over 200 3-wk-old mice screened from heterozygous parents, there were no homozygous deficient mice born.

PCR screening of embryos identified *PKC λ* -deficient embryos at day 8.5 (Fig. 3B) and day 9.5, but not at day 10 (Table I and data not shown). This result suggests that a deficiency in *PKC λ* during embryogenesis is lethal before day 9.5 and distinguishes *PKC λ* from all other PKC family members, including *PKC ζ* . Although embryos could be found through day 9.5, they were severely abnormal, as shown in the example of two day 9 embryos (Fig. 4). This is consistent with a role for aPKC in asymmetric cell divisions and embryo polarity as seen in *C. elegans* development (30).

To determine whether there was a transcript made in *PKC λ* ^{-/-} cells, RT-PCR was performed on RNA isolated from day 7.5 embryos (Fig. 3C). The primers amplify the entire coding region of the message, and we found no product in *PKC λ* ^{-/-} embryos using this strategy (Fig. 3C, lane 5).

Generation of *PKC λ* -deficient MEFs

To generate homozygous *PKC λ* -deficient ES cells, a second round of homologous recombination in the *PKC λ* ^{+/-} ES cells was induced with high doses of G418. The neomycin resistance gene used was shown to have a point mutation that decreases activity (40). A high concentration of G418 thus selects for clones with two copies of the targeting construct, and this apparently occurs at a reasonably high frequency by sister chromatid exchange. The original hemizygous ES cells were compared with clones selected with high G418 along with a cell line, P19, that is known to express *PKC λ* . Northern blot analysis using a 5' *PKC λ* -specific cDNA probe revealed a strong signal at the expected size of 4.5 kb in the P19 and hemizygous ES cells, but no detectable signal was found in the homozygous deficient cells (Fig. 3D). Although this seemed to establish that little or no message from the *PKC λ* locus was being made, we subsequently found that an aberrant message was present in *PKC λ* -deficient cells (see below; Fig. 3E).

C57BL/6-*PKC λ* ^{-/-} chimeric embryos were produced by injecting ES cells homozygous for the *PKC λ* mutant allele into 3.5-day

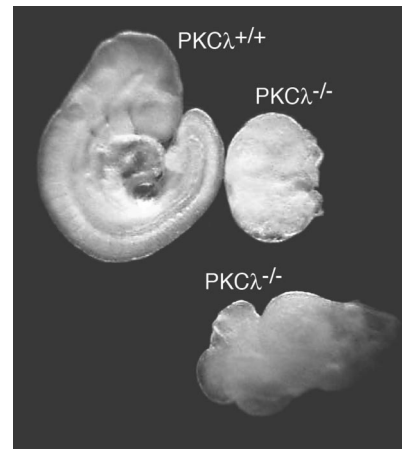


FIGURE 4. *PKC λ* -deficient embryos are morphologically abnormal. Embryos from day 9 timed matings of *PKC λ* ^{+/-} parents were photographed and typed by PCR for the mutant allele.

C57BL/6 blastocysts. MEFs were grown from day 13 and day 14 embryos, and the *PKC λ* -deficient MEFs were selected with G418. Fibroblasts were also isolated from *Rag2*^{-/-};*PKC λ* ^{+/-} chimeric mice and treated with G418 to serve as wild-type controls. The genotypes of the resulting MEFs were verified by PCR (data not shown). To further characterize the expression of *PKC λ* transcripts in deficient cells, the MEFs were immortalized using TAG. These cells were cloned and the genotype was verified.

To assess the state of *PKC λ* RNA expression transcribed from the mutant locus, we isolated RNA from the TAG MEFs and conducted RT-PCR. Primers were used that would detect messages transcribed from: exons 1–2 crossing intron 1; exons 1–6; exons 1–8; exon 9; exons 12–14; and exons 1–18 (Fig. 3E). We were able to amplify products using RNA from *PKC λ* ^{-/-} cells from exons upstream and downstream of the neo insertion, and as expected there was no product from exon 9. Curiously, there was also no product from exons 1–18. This could be due to absence of splicing between exons 8 and 11 that would be predicted to substantially increase the size of the transcript.

To compare levels of message from wild-type and *PKC λ* ^{-/-} cells, we performed real-time PCR. The average from three experiments showed that the aberrant 5' message produced from *PKC λ* ^{-/-} cells was 3.2-fold reduced compared with wild type (data not shown). These data indicate that the disrupted locus as diagramed in Fig. 1 does give rise to a message, albeit one that cannot encode a kinase-active enzyme. Most of the reactions span introns, and in addition, the minus reverse transcriptase controls in all reactions were always negative. As such, we can be sure that we were measuring cytoplasmic mRNA, and thus the primary transcript could be translated to produce an N-terminal polypeptide containing the protein interaction domains of *PKC λ* . Finally, we examined the protein expression of *PKC λ* in the primary MEFs using an Ab made against the catalytic domain, amino acids 397–558 (BD Transduction Laboratories). Consistent with the PCR analyses, no *PKC λ* was detectable in the deficient MEFs (Fig. 3F). From the following experiments, we can make conclusions concerning the kinase activity of *PKC λ* , but we cannot rule out the possibility that a reduced level of a polypeptide containing the protein-interacting domains influences the phenotype.

T cell development and function

Homozygous deficient ES cell clones were used to generate chimeric mice to analyze T cell development. As described above,

Table I. Genotype of progeny from intercrosses of *PKC λ* heterozygous mice

Age	Total	Genotype ^a		
		+/+	+/-	-/- ^b
3 wk	251	85	166	0
Ed ^c 16.5	7	4	3	0
Ed 14.5	7	2	5	0
Ed 9.5	21	9	9	3
Ed 8.5	44	13	22	7
Ed 7.5	93	19	60	14
Ed 7	44	15	19	10
Ed 6	69	26	37	6

^a Mice were genotyped by Southern blot or PCR using tail or embryo DNA.

^b All *PKC λ* ^{-/-} mice were morphologically abnormal.

^c Ed, Embryonic day.

chimeric mice were generated by the injection of the *PKC λ* -disrupted ES cells into either wild-type C57BL/6 or *Rag2*-deficient blastocysts. In the chimeras made with C57BL/6 blastocysts, *PKC λ* ^{-/-} and *PKC λ* ^{+/+} cells were distinguished by Ly9.1. Thymocytes and T cells from adult chimeric animals were analyzed for both lymphocyte subsets and T cell function. No changes were found in the CD4⁺ and CD8⁺ subpopulations from the thymus or from the peripheral lymphoid organs, indicating that a *PKC λ* deficiency does not cause a substantial disruption in T cell development (data not shown).

Basic T cell function was studied by measuring proliferation mediated by histoincompatible APCs (MLR) or mitogenic anti-TCR stimulation. We also measured cytotoxic T cell activity by inducing CTLs to the histoincompatible P815 tumor. In none of these assays did we detect a difference in the response elicited in wild-type vs *PKC λ* -deficient T cells. An example is shown in Fig. 5. Splenocytes from a wild-type mouse were compared with splenocytes from two *PKC λ* ^{-/-};*Rag2*^{-/-} chimeras, where the only T cells and B cells present are *PKC λ* deficient. Plate-bound anti-CD3 was titrated into culture alone or in the presence of costimulation in the form of anti-CD28 Ab or the cytokine IL-2. As shown, the proliferation of the wild-type and *PKC λ* -deficient T cells was identical. These basic analyses of T cell development and activation do not rule out the possibility that *PKC λ* plays a role in some form of a T cell-mediated immune response, but they do indicate that the basic processes of signal transduction leading to proliferation and cytotoxic effector T cells are intact.

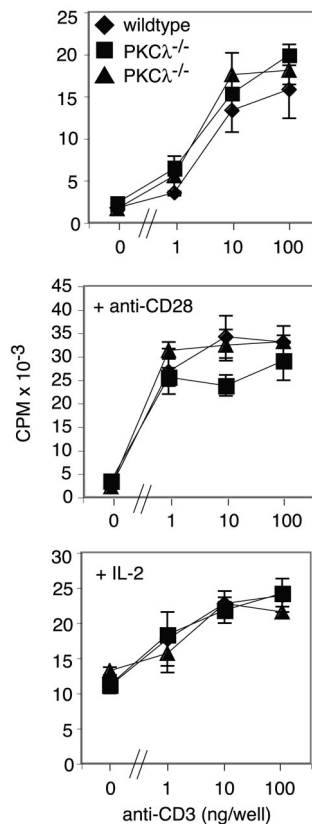


FIGURE 5. T cell proliferation is normal in the absence of *PKC λ* . Splenocytes from a wild-type mouse or two *PKC λ* ^{-/-};*Rag2*^{-/-} chimeras (*PKC λ* ^{-/-}) were cultured with plate-bound anti-CD3 alone (*top panel*) or in the presence of soluble anti-CD28 (*middle panel*) or rIL-2 (*bottom panel*) for 3 days. Proliferation was assessed by tritiated thymidine incorporation during the last 18 h of incubation. Six chimeras and 20 fetal liver chimeras were analyzed with similar results.

PKC λ -deficient MEFs exhibit alterations in morphology and actin stress fibers

The growth characteristics of wild-type and *PKC λ* -deficient MEFs were variable, but we did not detect a consistent difference. However, a striking difference between the wild-type and *PKC λ* -deficient cells was an increase in the overall cell size as determined by microscopic examination and flow cytometric analysis (data not shown).

To investigate a potential basis for this difference, fluorescence microscopy was used to analyze the cytoskeleton of MEFs grown in medium containing 10% serum. Actin stress fibers, the adhesion plaque protein paxillin, vimentin, and microtubules were visualized in wild-type and mutant MEFs. Staining of F-actin with phalloidin revealed that the mutant cells had a higher abundance of stress fibers than did wild-type cells (compare Fig. 6, *A* and *C*, with Fig. 6, *B* and *D*). Likewise, immunostaining for paxillin revealed more potential focal adhesion contacts in the mutant cells (Fig. 6*B*) than in the wild-type cells (Fig. 6*A*). The intermediate filaments showed the typical splayed pattern in both cell types (Fig. 6, *C* and *D*), although in the mutant cells their distribution seemed to more closely follow the linear pattern of stress fibers (Fig. 6*D*). The

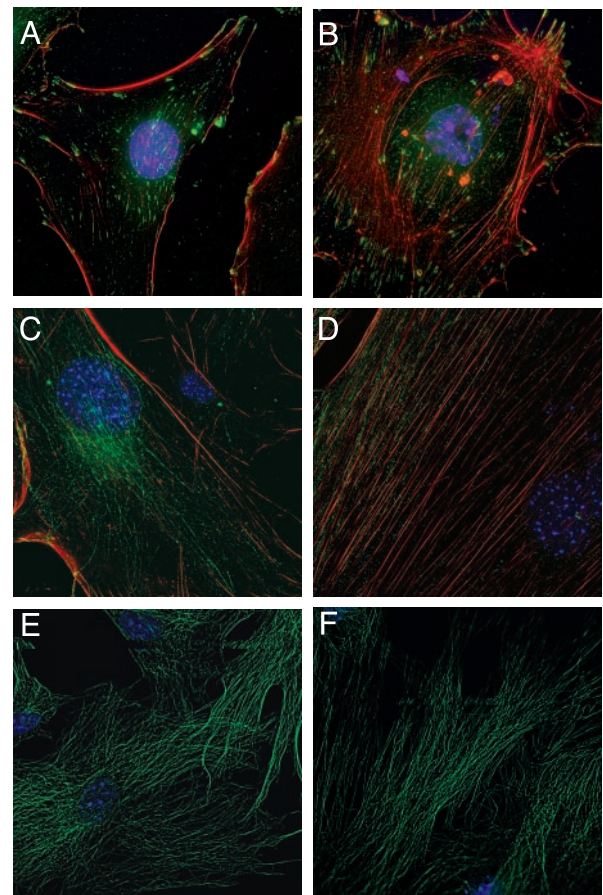


FIGURE 6. Alteration of the actin stress fibers in *PKC λ* -deficient fibroblasts. MEFs were grown on coverslips in medium with 10% serum. After the cells were fixed and permeabilized, they were labeled with fluorescent proteins and Abs specific for actin, paxillin, vimentin, and tubulin. *A* and *B*, MEFs stained with tetramethylrhodamine isothiocyanate-phalloidin (red), anti-paxillin (green), and 4',6'-diamidino-2-phenylindole (blue); $\times 40$ magnification. *C* and *D*, $\times 60$ magnification of MEFs stained with phalloidin (red), anti-vimentin (green), and Hoechst (blue). *E* and *F*, MEFs stained with anti-tubulin (green) and Hoechst (blue) at $\times 40$ magnification. *A*, *C*, and *E*, Wild-type MEFs. *B*, *D*, and *F*, *PKC λ* -deficient MEFs. These experiments were repeated three times on two cell lines per genotype.

microtubules (Fig. 6, *E* and *F*) and their organization centers appeared normal in both cell types as well. These data are in concert with findings that PKC λ associates with Cdc42 and mediates the loss of stress fibers (41).

TNF-mediated activation of ERK and NF- κ B

To determine the requirements for PKC λ in signaling cascades, immortalized PKC λ -deficient MEFs were compared with wild-type MEFs. One proposed role for aPKCs is the activation of ERK after stimulation with serum or TNF. In COS-1 cells given either stimulus, ERK is activated, and this can be blocked by the overexpression of kinase-dead PKC λ or PKC ζ (4, 15, 42). To ascertain whether activation of the ERK signaling pathway requires PKC λ , wild-type and PKC λ -deficient TAG fibroblasts were serum starved for 48 h and then stimulated with TNF, EGF, serum, or PMA plus calcium ionophore for 15 min. The PMA plus calcium ionophore treatment served as a positive control because this treatment was shown to activate ERK in an aPKC-independent manner. In the experiment depicted in Fig. 7A, ERK1 and ERK2 were phosphorylated in both wild-type and PKC λ -deficient MEFs by EGF, serum, and PMA plus ionomycin. Stimulation with TNF was also found to be unchanged (Fig. 7B). These data demonstrate that PKC λ is not essential for the activation of ERK in fibroblasts.

Studies using pharmacological inhibitors or dominant interfering mutants also suggest that aPKC in general, and PKC λ in particular, activates NF- κ B after TNF stimulation (16, 18, 43, 44). To assess the role of PKC λ in these signaling pathways, we conducted two types of experiments that assay NF- κ B activation. In the first, wild-type and PKC λ -deficient TAG fibroblasts were activated with TNF, and the levels of I κ B were assessed over time by Western blotting. The amount of I κ B decreased ~20-fold for both wild-type and mutant cells with identical kinetics (Fig. 8).

In a second type of experiment, wild-type and PKC λ -deficient cells were cotransfected with a luciferase reporter construct driven by three NF- κ B binding sites along with a constitutively active

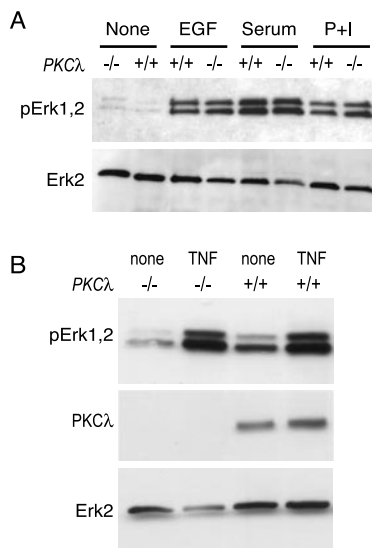


FIGURE 7. The TNF- α and ERK signaling pathways in PKC λ -deficient fibroblasts are intact. *A*, Immortalized MEFs were stimulated with EGF, serum, or PMA plus calcium ionophore for 15 min. ERK activation was determined by pERK Western blot. Equal loading was confirmed by detection of total ERK2. *B*, TAG-immortalized MEFs were stimulated with TNF- α for 15 min. Cell lysates were analyzed by Western blot for phosphorylated ERK1, phosphorylated ERK2, PKC λ , and ERK2. These experiments were repeated three to five times.

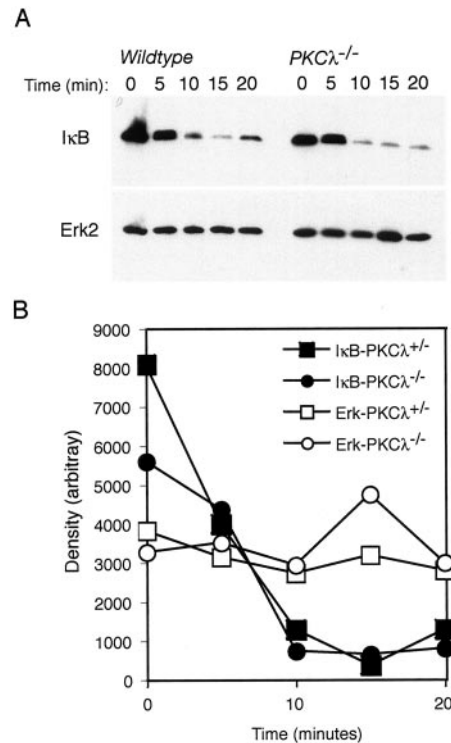


FIGURE 8. Degradation of I κ B α is normal in response to TNF. *A*, TAG MEFs were stimulated with TNF for 0 to 20 min, and cells were harvested at 5-min intervals. The degradation of I κ B α was determined by Western blot analysis with an anti-I κ B α specific Ab. Total ERK2 was detected as a control for equal loading. This experiment was repeated three times. *B*, Densitometric analysis of the I κ B α and ERK signals demonstrates that I κ B α was degraded with the same kinetics in both wild-type and PKC λ -deficient cells.

renilla luciferase plasmid as a control for transfection efficiency. After stimulation with TNF or PMA, NF- κ B activity was assessed by the ratio of luciferase to renilla luciferase (Fig. 9A), and the fold stimulation is listed for four consecutive experiments (Fig. 9B). As shown, the activation of NF- κ B by TNF in the PKC λ -deficient cells was not significantly different. Thus, by two criteria, we found no defect in the ability of cells deficient for PKC λ to respond to TNF as measured by the activation of NF- κ B. In light of these data, then perhaps it is not surprising that there was no defect detected in T cell development and activation. Although we did not examine NF- κ B signaling in T cells directly, we would expect that this would have been readily revealed by T cell activation experiments.

Drosophila aPKC has been shown to be required for the Toll-mediated activation of the NF- κ B orthologs Dif and Dorsal (45). To investigate TLR-mediated responses, we stimulated transformed wild-type and PKC λ -deficient MEFs with LPS, IL-1 β , or PMA and assayed for NF- κ B activity using the luciferase reporter described above (Fig. 9C). As shown, these responses were also indistinguishable between the two cell types.

The conclusion from the experiments described above is that PKC λ is dispensable for the TNF- or TLR-mediated induction of NF- κ B; however, one potential caveat is that in the absence of PKC λ , there could be a compensatory overexpression of PKC ζ . The logic would be that a level of aPKC is required that can be satisfied by either PKC ζ or PKC λ . To study this, extracts from transformed MEFs were separated by electrophoresis and analyzed by immunoblotting. An extract from the human A431 carcinoma, provided by the manufacturer as a control for PKC ζ expression,

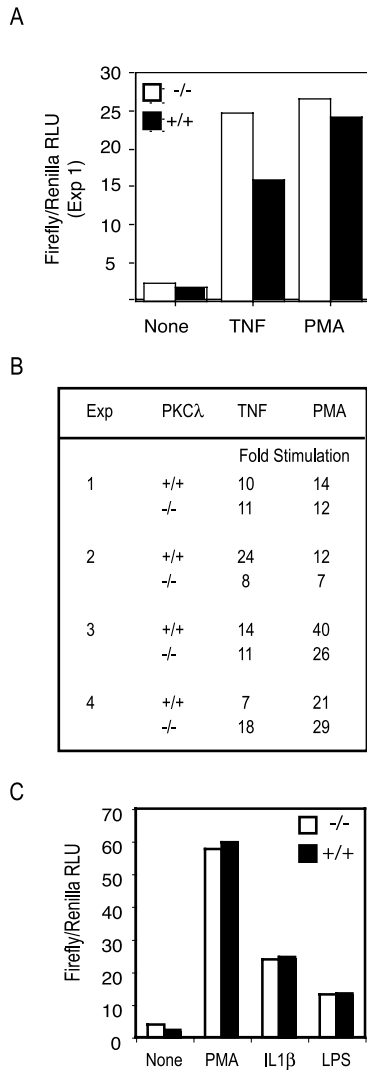


FIGURE 9. Normal activation of NF- κ B in *PKC λ ^{-/-}* cells. **A**, Immortalized MEFs were transfected with a 3(HIV) κ B-firefly luciferase reporter construct and constitutively expressed renilla luciferase as a control for transfection efficiency. The cells were stimulated with TNF or PMA for 2 h at 48 h posttransfection. The induction of NF- κ B is expressed as firefly relative light units divided by the renilla relative light units. **B**, Results of four consecutive experiments. **C**, TAG MEFs were transfected with the 3(HIV) κ B-firefly luciferase reporter construct and renilla luciferase. Forty-eight hours later, the cells were stimulated with PMA, IL-1 β , or LPS for 2 h and luciferase activity was assessed. Open bars, *PKC λ ^{-/-}* cells; filled bars, wild-type cells.

was included. Ab made to a polypeptide immunogen corresponding to PKC λ amino acids 397–558 revealed a single band that was absent in the *PKC λ* -deficient MEFs, as expected (Fig. 10, top panel). According to molecular mass markers, PKC λ exhibits an electrophoretic mobility corresponding to ~70 kDa, whereas its predicted molecular mass based on amino acid sequence is 67.6 kDa. Polyclonal Ab made to a 16-aa carboxy-terminal peptide from rat/mouse PKC ζ was also tested. This peptide is identical with the orthologous peptide found in PKC λ at 14/16 positions. As shown, there is a strong band that apparently corresponds to PKC λ in that it is absent in the *PKC λ* -deficient MEFs (Fig. 10, bottom panel). The Ab therefore cross-reacts with PKC ζ and PKC λ . Because PKC ζ has a predicted molecular mass (67.2 kDa) and isoelectric point almost identical with PKC λ , these cytoplasmic proteins, not known to be posttranslationally modified in unactivated

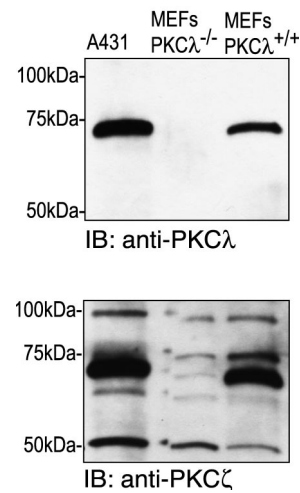


FIGURE 10. Expression of PKC λ and PKC ζ in immortalized MEFs. Extracts from MEFs were resolved by SDS-PAGE and blotted as described in *Materials and Methods*. Immunoblotting was conducted using rabbit anti-PKC ζ (07-264; Upstate Biotechnology) or mouse anti-PKC λ (610208; BD Transduction Laboratories). Secondary developing Abs were from Vector Laboratories.

cells, are not likely to exhibit significantly different electrophoretic mobility. A faint band at 70 kDa seen in *PKC λ* -deficient cells presumably corresponds to PKC ζ , but clearly there is no overexpression of PKC ζ that could compensate for the high level of PKC λ found in wild-type MEFs. We note that this similarity in electrophoretic mobility and the cross-reactivity using commercially available Abs has probably contributed to the confusion in the literature regarding the function of these different aPKC molecules.

Discussion

The aPKCs have been implicated in several fundamental cellular processes including embryo polarity, asymmetric cell division, NF- κ B activation, and survival. In this report, we provide evidence that, in mammals, these functions are distributed between the two aPKC molecules, PKC ζ and PKC λ . PKC λ is essential for embryogenesis and cytoskeletal function, whereas it is not essential for TNF-, IL-1-, or LPS-mediated activation.

Of significant interest is the requirement for *PKC λ* in the normal development of mouse embryos. *PKC λ* -deficient embryos die by day 9.5. At this time point the mutant embryos are shrunken and lacking in any recognizable structures (Fig. 4), with abnormalities seen as early as day 6.5. This phenotype is in agreement with that found for the disrupted expression of the aPKC orthologs in *C. elegans* (30), *Xenopus* (12, 42), and *Drosophila* (46–49). Functional knockouts in these organisms result in early embryo lethality. In the absence of the *C. elegans* ortholog PKC-3, asymmetric divisions of the blastomeres are disrupted, resulting in defects in embryo polarity (30). *Drosophila* aPKC, the *Drosophila* homologue, has also been shown to regulate oocyte polarity (45, 47) and asymmetric cell division (48, 49). Similarly, when PKC λ function is abrogated in *Xenopus* oocytes, mitogenesis and oocyte maturation are inhibited (12, 42). Similarly, we have shown that the germline disruption of PKC λ results in early embryo lethality. This is the first mammalian PKC isoform to be identified as an essential component of early development, and this result specifically shows that the two atypical PKC isoforms are not redundant in this regard. Whether the embryo lethality is due to defects in establishing embryo polarity is a topic for further investigation.

PKC λ is also essential for normal cellular morphology in fibroblasts. We found a greater abundance of actin stress fibers in the mutant cells compared with wild-type cells. In a subset of mutant cells (Fig. 6B), but not wild-type cells (Fig. 6A), the actin fibers appeared radial. This is of interest because the aPKCs have been linked to the regulation of the actin cytoskeleton by their interaction with the GTP binding protein Cdc42 via PAR-6, a scaffolding protein (41, 50–53). The regulation of the actin cytoskeleton by Cdc42 and its associated proteins is complex, as is its regulation of cell growth (54). Whether the observed stress fiber phenotype is related to an effect on Cdc42 activity or expression is unknown, but should be an avenue for future study. We propose that PKC λ is involved in the steady state regulation of actin assembly or disassembly, and potentially in focal adhesion contacts. In its absence, there also appeared to be more localization of paxillin in focal contacts. Similarly, although PKC λ did not appear to dramatically alter intermediate filament distribution, a subtle change could be seen. Whether this is simply due to the greater abundance of actin stress fibers in the mutant cells or to the reported role of Cdc42 in intermediate filament distribution (55) is not clear at this time. In contrast, the distribution of microtubules and the organization center was unaffected by the absence of PKC λ , as determined by tubulin staining.

The aPKC proteins have been reported to be intermediates in TNF signaling pathways such that the inhibition of the aPKC activity by overexpression of kinase-dead PKC ζ or PKC λ mutants resulted in disruption of ERK and NF- κ B activation after TNF treatment (14–18, 56). In addition, the single aPKCs present in invertebrates appears to play a role in both embryo polarity and signaling, leading to the activation of NF- κ B family members. Despite our expectation that PKC λ -deficient cells would exhibit a similar lack of a TNF response, our experiments demonstrate that PKC λ is not an essential component in these signaling pathways. TNF-induced ERK and NF- κ B activation were unchanged in the PKC λ -deficient fibroblasts, and EGF activation of ERK was unaltered as well. PKC λ may participate in this signaling, but it is not necessary.

We did find that mRNA originating from the mutant locus is present in the TAG MEFs at about a 3-fold decrease compared with wild-type TAG MEFs. We determined that this message could give rise to a polypeptide including the N-terminal interaction domains, but lacking the catalytic site present in the deleted exon 9 (Fig. 3E). As such, we can conclude that NF- κ B and ERK responses induced by the indicated agents do not require kinase activity from PKC λ . The translation product that could potentially result from the disrupted locus, if anything, would be expected to mediate protein interactions and act as a dominant interfering form of aPKC.

PKC ζ -deficient mice develop normally, with the exception of phenotypic differences in the Peyer's patches and spleens that are similar to the TNF receptor-1 and the lymphotoxin- β receptor-deficient mice (19). MEFs from PKC ζ -deficient animals are defective in their activation of NF- κ B after TNF and IL-1 stimulation, and thus, in combination with the results presented here, we would conclude that the requirement for aPKC in NF- κ B responses previously elucidated by experiments using dominant interfering aPKC constructs is PKC ζ specific. The activation of ERK in the PKC ζ -deficient cells was normal, and therefore neither aPKC is necessary for activation of ERK in fibroblasts after TNF treatment.

The source of the discrepancy between the results presented in this report and the previously published work cited above may be due to the lack of specificity in Abs, pharmacological inhibitors, or kinase-dead dominant interfering forms of the kinase. We find it

surprising that all of these studies would mistakenly implicate PKC λ in NF- κ B activation and survival, but we find no other explanation. Conversely, PKC ζ has been published as a part of the Cdc42/Rac1-PAR6 polarity complex (52, 57), whereas the relevant isoform may be PKC λ . Although we have not addressed this directly, we note that PKC ζ -deficient mice are grossly normal, with defects limited to secondary lymphoid organs, whereas PKC λ -deficient mice show early embryonic disorganization (Fig. 4).

In light of the lack of an effect on NF- κ B activation, it is perhaps not surprising that we found T cell development and activation to be normal for PKC λ -defective T cells. In the absence of NF- κ B activation, Ag-activated T cells undergo p73-induced apoptosis (58). If PKC λ was important for inducing NF- κ B, we reasoned that we would see an effect on T cell proliferation and accumulation. In addition, we were interested in the ability of T cells to form the cellular interactions necessary for CTL activity, and again we found that the absence of PKC λ had no discernable effect. It is quite possible that the tissue culture-based experiments that we performed missed effects on the T cell activation and survival associated with a natural immune response *in vivo*; however, this will have to be resolved using conditional knockout mice.

Invertebrates have only a single atypical PKC to perform the seemingly disparate functions of signaling emanating from cytokine receptors and TLRs as well as mediating embryo polarity and asymmetric cell divisions. The commonality of these functions in signaling have yet to be determined; however, mice (and in all likelihood other vertebrates) appear to have segregated these functions into PKC ζ and PKC λ . More investigation is required to identify the pathways mediated by PKC λ that control normal embryogenesis, cytoskeleton organization, and perhaps cell polarity.

Acknowledgments

We thank Yang Xu for his expert and generous help in preparing RAG2 blastocyst chimeras and Randall Johnson, John Earle, Carolan Buckmaster, Michelle Paulus, Nissi Varki, and Leslie Sharp for technical expertise and assistance. We also thank Irene Ch'en and Tom Nugent for critical reviews of the manuscript.

References

- Nishizuka, Y. 1995. Protein kinase C and lipid signaling for sustained cellular responses. *FASEB J.* 9:484.
- Exton, J. H. 1994. Phosphatidylcholine breakdown and signal transduction. *Biochim. Biophys. Acta* 1212:26.
- Akimoto, K., K. Mizuno, S. Osada, S. Hirai, S. Tanuma, K. Suzuki, and S. Ohno. 1994. A new member of the third class in the protein kinase C family, PKC λ , expressed dominantly in an undifferentiated mouse embryonal carcinoma cell line and also in many tissues and cells. *J. Biol. Chem.* 269:12677.
- Akimoto, K., R. Takahashi, S. Moriya, N. Nishioka, J. Takayanagi, K. Kimura, Y. Fukui, S. Osada, K. Mizuno, S. Hirai, A. Kazlauskas, and S. Ohno. 1996. EGF or PDGF receptors activate atypical PKC- λ through phosphatidylinositol 3-kinase. *EMBO J.* 15:788.
- Selbie, L. A., C. Schmitz-Peiffer, Y. Sheng, and T. J. Biden. 1993. Molecular cloning and characterization of PKC ι , an atypical isoform of protein kinase C derived from insulin-secreting cells. *J. Biol. Chem.* 268:24296.
- Diaz-Meco, M. T., J. Lozano, M. M. Municio, E. Berra, S. Frutos, L. Sanz, and J. Moscat. 1994. Evidence for the *in vitro* and *in vivo* interaction of Ras with protein kinase C ζ . *J. Biol. Chem.* 269:31706.
- Bareggi, R., V. Grill, M. Zweyer, P. Narducci, and A. M. Martelli. 1995. Distribution of the extended family of protein kinase C isoenzymes in fetal organs of mice: an immunohistochemical study. *Cell Tissue Res.* 280:617.
- Goodnight, J., M. G. Kazanietz, P. M. Blumberg, J. F. Mushinski, and H. Mischak. 1992. The cDNA sequence, expression pattern and protein characteristics of mouse protein kinase C- ζ . *Gene* 122:305.
- Rybin, V. O., P. M. Buttrick, and S. F. Steinberg. 1997. PKC- λ is the atypical protein kinase C isoform expressed by immature ventricle. *Am. J. Physiol.* 272:H1636.
- Jiang, Y. H., J. R. Lupton, and R. S. Chapkin. 1997. Dietary fat and fiber modulate the effect of carcinogen on colonic protein kinase C λ expression in rats. *J. Nutr.* 127:1938.
- Murray, N. R., and A. P. Fields. 1997. Atypical protein kinase C ι protects human leukemia cells against drug-induced apoptosis. *J. Biol. Chem.* 272:27521.

12. Dominguez, I., M. T. Diaz-Meco, M. M. Municio, E. Berra, A. Garcia de Herreros, M. E. Cornet, L. Sanz, and J. Moscat. 1992. Evidence for a role of protein kinase C ζ subspecies in maturation of *Xenopus laevis* oocytes. *Mol. Cell. Biol.* 12:3776.
13. Dominguez, I., L. Sanz, F. Arenzana-Seisdedos, M. T. Diaz-Meco, J. L. Virelizier, and J. Moscat. 1993. Inhibition of protein kinase C ζ subspecies blocks the activation of an NF- κ B-like activity in *Xenopus laevis* oocytes. *Mol. Cell. Biol.* 13:1290.
14. Berra, E., M. T. Diaz-Meco, J. Lozano, S. Frutos, M. M. Municio, P. Sanchez, L. Sanz, and J. Moscat. 1995. Evidence for a role of MEK and MAPK during signal transduction by protein kinase C ζ . *EMBO J.* 14:6157.
15. Kampfer, S., K. Hellbert, A. Villunger, W. Doppler, G. Baier, H. H. Grunicke, and F. Uberall. 1998. Transcriptional activation of *c-fos* by oncogenic Ha-Ras in mouse mammary epithelial cells requires the combined activities of PKC- λ , ϵ and ζ . *EMBO J.* 17:4046.
16. Bonizzi, G., J. Piette, S. Schoonbroodt, M. P. Merville, and V. Bours. 1999. Role of the protein kinase C λ/ι isoform in nuclear factor- κ B activation by interleukin-1 β or tumor necrosis factor- α : cell type specificities. *Biochem. Pharmacol.* 57:713.
17. Sanz, L., P. Sanchez, M. J. Lallena, M. T. Diaz-Meco, and J. Moscat. 1999. The interaction of p62 with RIP links the atypical PKCs to NF- κ B activation. *EMBO J.* 18:3044.
18. Lallena, M. J., M. T. Diaz-Meco, G. Bren, C. V. Paya, and J. Moscat. 1999. Activation of I κ B kinase β by protein kinase C isoforms. *Mol. Cell. Biol.* 19:2180.
19. Leitges, M., L. Sanz, P. Martin, A. Duran, U. Braun, J. F. Garcia, F. Camacho, M. T. Diaz-Meco, P. D. Rennett, and J. Moscat. 2001. Targeted disruption of the ζ PKC gene results in the impairment of the NF- κ B pathway. *Mol. Cell* 8:771.
20. Ito, T., Y. Matsui, T. Ago, K. Ota, and H. Sumimoto. 2001. Novel modular domain PB1 recognizes PC motif to mediate functional protein-protein interactions. *EMBO J.* 20:3938.
21. Watts, J. L., B. Etemad-Moghadam, S. Guo, L. Boyd, B. W. Draper, C. C. Mello, J. R. Priess, and K. J. Kemphues. 1996. par-6, a gene involved in the establishment of asymmetry in early *C. elegans* embryos, mediates the asymmetric localization of PAR-3. *Development* 122:3133.
22. Suzuki, A., T. Yamanaka, T. Hirose, N. Manabe, K. Mizuno, M. Shimizu, K. Akimoto, Y. Izumi, T. Ohnishi, and S. Ohno. 2001. Atypical protein kinase C is involved in the evolutionarily conserved par protein complex and plays a critical role in establishing epithelia-specific junctional structures. *J. Cell Biol.* 152:1183.
23. Sanchez, P., G. De Carcer, I. V. Sandoval, J. Moscat, and M. T. Diaz-Meco. 1998. Localization of atypical protein kinase C isoforms into lysosome-targeted endosomes through interaction with p62. *Mol. Cell. Biol.* 18:3069.
24. Puls, A., S. Schmidt, F. Grawe, and S. Stabel. 1997. Interaction of protein kinase C ζ with ZIP, a novel protein kinase C-binding protein. *Proc. Natl. Acad. Sci. USA* 94:6191.
25. Suzuki, A., K. Akimoto, and S. Ohno. 2003. Protein kinase C λ/ι (PKC λ/ι): a PKC isotype essential for the development of multicellular organisms. *J. Biochem.* 133:9.
26. Lamark, T., M. Perander, H. Outzen, K. Kristiansen, A. Overvatn, E. Michaelsen, G. Bjorkoy, and T. Johansen. 2003. Interaction codes within the family of mammalian Phox and Bem1p domain-containing proteins. *J. Biol. Chem.* 278:34568.
27. Wooten, M. W., M. L. Vandenplas, M. L. Seibenhener, T. Geetha, and M. T. Diaz-Meco. 2001. Nerve growth factor stimulates multisite tyrosine phosphorylation and activation of the atypical protein kinase C's via a Src kinase pathway. *Mol. Cell. Biol.* 21:8414.
28. Diaz-Meco, M. T., M. M. Municio, S. Frutos, P. Sanchez, J. Lozano, L. Sanz, and J. Moscat. 1996. The product of par-4, a gene induced during apoptosis, interacts selectively with the atypical isoforms of protein kinase C. *Cell* 86:777.
29. Sells, S. F., S. S. Han, S. Muthukkumar, N. Maddiwar, R. Johnstone, E. Boghaert, D. Gillis, G. Liu, P. Nair, S. Monnig, et al. 1997. Expression and function of the leucine zipper protein Par-4 in apoptosis. *Mol. Cell. Biol.* 17:3823.
30. Tabuse, Y., Y. Izumi, F. Piano, K. J. Kemphues, J. Miwa, and S. Ohno. 1998. Atypical protein kinase C cooperates with PAR-3 to establish embryonic polarity in *Caenorhabditis elegans*. *Development* 125:3607.
31. Soriano, P., C. Montgomery, R. Geske, and A. Bradley. 1991. Targeted disruption of the *c-src* proto-oncogene leads to osteopetrosis in mice. *Cell* 64:693.
32. Chun, J. J., D. G. Schatz, M. A. Oettinger, R. Jaenisch, and D. Baltimore. 1991. The recombination activating gene-1 (RAG-1) transcript is present in the murine central nervous system. *Cell* 64:189.
33. Tevethia, M. J., H. A. Lacko, and A. Conn. 1998. Two regions of simian virus 40 large T-antigen independently extend the life span of primary C57BL/6 mouse embryo fibroblasts and cooperate in immortalization. *Virology* 243:303.
34. Kaye, J., M. L. Hsu, M. E. Sauron, S. C. Jameson, N. R. Gascoigne, and S. M. Hedrick. 1989. Selective development of CD4⁺ T cells in transgenic mice expressing a class II MHC-restricted antigen receptor. *Nature* 341:746.
35. Isakov, N., and A. Altman. 1987. Human T lymphocyte activation by tumor promoters: role of protein kinase C. *J. Immunol.* 138:3100.
36. Agard, D. A., Y. Hiraoka, P. Shaw, and J. W. Sedat. 1989. Fluorescence microscopy in three dimensions. *Methods Cell Biol.* 30:353.
37. Mochly-Rosen, D., and A. S. Gordon. 1998. Anchoring proteins for protein kinase C: a means for isozyme selectivity. *FASEB J.* 12:35.
38. Abeliovich, A., R. Paylor, C. Chen, J. J. Kim, J. M. Wehner, and S. Tonegawa. 1993. PKC γ mutant mice exhibit mild deficits in spatial and contextual learning. *Cell* 75:1263.
39. Hentze, M. W., and A. E. Kulozik. 1999. A perfect message: RNA surveillance and nonsense-mediated decay. *Cell* 96:307.
40. Yenofsky, R. L., M. Fine, and J. W. Pellow. 1990. A mutant neomycin phosphotransferase II gene reduces the resistance of transformants to antibiotic selection pressure. *Proc. Natl. Acad. Sci. USA* 87:3435.
41. Coghlan, M. P., M. M. Chou, and C. L. Carpenter. 2000. Atypical protein kinases C- λ and - ζ associate with the GTP-binding protein Cdc42 and mediate stress fiber loss. *Mol. Cell. Biol.* 20:2880.
42. Berra, E., M. T. Diaz-Meco, I. Dominguez, M. M. Municio, L. Sanz, J. Lozano, R. S. Chapkin, and J. Moscat. 1993. Protein kinase C ζ isoform is critical for mitogenic signal transduction. *Cell* 74:555.
43. Wooten, M. W. 1999. Function for NF- κ B in neuronal survival: regulation by atypical protein kinase C. *J. Neurosci. Res.* 58:607.
44. Wooten, M. W., M. L. Seibenhener, V. Mamidipudi, M. T. Diaz-Meco, P. A. Barker, and J. Moscat. 2001. The atypical protein kinase C-interacting protein p62 is a scaffold for NF- κ B activation by nerve growth factor. *J. Biol. Chem.* 276:7709.
45. Avila, A., N. Silverman, M. T. Diaz-Meco, and J. Moscat. 2002. The Drosophila atypical protein kinase C-ref(2)p complex constitutes a conserved module for signaling in the toll pathway. *Mol. Cell. Biol.* 22:8787.
46. Wodarz, A., A. Ramrath, A. Grimm, and E. Knust. 2000. Drosophila atypical protein kinase C associates with Bazooka and controls polarity of epithelia and neuroblasts. *J. Cell Biol.* 150:1361.
47. Cox, D. N., S. A. Seyfried, L. Y. Jan, and Y. N. Jan. 2001. Bazooka and atypical protein kinase C are required to regulate oocyte differentiation in the Drosophila ovary. *Proc. Natl. Acad. Sci. USA* 98:14475.
48. Cai, Y., F. Yu, S. Lin, W. Chia, and X. Yang. 2003. Apical complex genes control mitotic spindle geometry and relative size of daughter cells in Drosophila neuroblast and pI asymmetric divisions. *Cell* 112:51.
49. Betschinger, J., K. Mechtler, and J. A. Knoblich. 2003. The Par complex directs asymmetric cell division by phosphorylating the cytoskeletal protein Lgl. *Nature* 422:326.
50. Izumi, Y., T. Hirose, Y. Tamai, S. Hirai, Y. Nagashima, T. Fujimoto, Y. Tabuse, K. J. Kemphues, and S. Ohno. 1998. An atypical PKC directly associates and colocalizes at the epithelial tight junction with ASIP, a mammalian homologue of *Caenorhabditis elegans* polarity protein PAR-3. *J. Cell Biol.* 143:95.
51. Uberall, F., K. Hellbert, S. Kampfer, K. Maly, A. Villunger, M. Spitaler, J. Mwanjewe, G. Baier-Bitterlich, G. Baier, and H. H. Grunicke. 1999. Evidence that atypical protein kinase C- λ and atypical protein kinase C- ζ participate in Ras-mediated reorganization of the F-actin cytoskeleton. *J. Cell Biol.* 144:413.
52. Qiu, R. G., A. Abo, and G. Steven Martin. 2000. A human homolog of the *C. elegans* polarity determinant Par-6 links Rac and Cdc42 to PKC ζ signaling and cell transformation. *Curr. Biol.* 10:697.
53. Joberty, G., C. Petersen, L. Gao, and I. G. Macara. 2000. The cell-polarity protein Par6 links Par3 and atypical protein kinase C to Cdc42. *Nat. Cell Biol.* 2:531.
54. Erickson, J. W., and R. A. Cerione. 2001. Multiple roles for Cdc42 in cell regulation. *Curr. Opin. Cell Biol.* 13:153.
55. Chan, W., R. Kozma, Y. Yasui, M. Inagaki, T. Leung, E. Manser, and L. Lim. 2002. Vimentin intermediate filament reorganization by Cdc42: involvement of PAK and p70 S6 kinase. *Eur. J. Cell Biol.* 81:692.
56. Anthonen, M. W., S. Andersen, A. Solhaug, and B. Johansen. 2001. Atypical λ/ι PKC conveys 5-lipoxygenase/leukotriene B₄-mediated cross-talk between phospholipase A₂s regulating NF- κ B activation in response to tumor necrosis factor- α and interleukin-1 β . *J. Biol. Chem.* 276:35344.
57. Wang, H. R., Y. Zhang, B. Ozdamar, A. A. Ogunjimi, E. Alexandrova, G. H. Thomsen, and J. L. Wrana. 2003. Regulation of cell polarity and protrusion formation by targeting RhoA for degradation. *Science* 302:1775.
58. Wan, Y. Y., and J. DeGregori. 2003. The survival of antigen-stimulated T cells requires NF κ B-mediated inhibition of p73 expression. *Immunity* 18:331.